DOI: 10.1002/ejic.200901083

Self-Assembled Lanthanide Salicylaldimines with a Unique Coordination Mode

Małgorzata T. Kaczmarek,[a] Maciej Kubicki,[a] Anna Mondry,[b] Rafał Janicki,[b] and Wanda Radecka-Paryzek*[a]

Keywords: Self-assembly / Lanthanides / Schiff bases / O ligands / Coordination modes

New lanthanide salicylaldimine complexes of the formula $[Ln(H_2L)_3(NO_3)_3](H_2L)$, where Ln = La^{3+} (**1**), Nd^{3+} (**2**), Eu^{3+} (**3**), Gd^{3+} (**4**), Ho^{3+} (**5**), Er^{3+} (**6**), Tb^{3+} (**7**) or Yb^{3+} (**8**), and H_2L = *N*,*N*′-bis(salicylidene)-4-methyl-1,3-phenylenediamine, were formed in a self-assembly process involving the lanthanide template-induced one-step [2+1] Schiff base condensation reaction between salicylaldehyde and 4-methyl-1,3-phenylenediamine. The unusual coordination pattern of salen-type ligands in these complexes, in which the three potentially tetradentate N_2O_2 salicylaldimines function as undeprotonated, monodentate, exclusively O-donor ligands without involving the nitrogen atoms in the coordination environment, was proved by single-crystal X-ray diffraction analysis and correlated with spectroscopic characterization. In this species with the nine-coordinate distorted tricapped trigonal prism geometry, the nitrates act as bidentate chelators occupying six coordination sites and leaving the remaining sites available for salicylaldimine ligands formed in situ in the template process. The additional salicylaldimine molecule acts as a guest for the salicylaldimine complex host and stabilizes the overall self-assembled supramolecular network.

Introduction

The importance of Schiff base complexes for bioinorganic chemistry, biomedical application, supramolecular chemistry, catalysis and materials science, separation and encapsulation processes, and the formation of compounds with unusual properties and structures has been well recognized and reviewed.[1] Among them, salicylaldimine (salen-type) Schiff base complexes derived from salicylaldehyde and various diamines attract considerable attention, because they can be used as enantioselective epoxidation catalysts;[2] components for the assembly of supramolecular architectures displaying interesting structures and properties;[3] as models for active sites of metalloenzymes; as fluorogenic, pesticide, and herbicidal agents; and therapeutics with antibacterial, antiviral, and antifungal properties and superoxide dismutase and catalase activity.[4] X-ray structure data reveal that in the d block metal salicylaldimine complexes, Schiff bases generally act as deprotonated tetradentate ligands with the N_2O_2 set of donor atoms capable of effective coordination in the planar fashion.[1,5] Compared with d block complexes, only a few structures of salicylaldimine complexes of 4f block metal ions (lanthanides) are known. They display dianionic tetradentate N_2O_2 arrangement of donor atoms around the lanthanide ions.[6] In view of the potential application of the lanthanide complexes in chemistry, biochemistry, medicine, and technology,[7] and continuing our interest in the investigation of the coordination template effect in generating supramolecular polyaza and polyoxaaza lanthanide Schiff bases, we have recently reported the definitive structural details of a salicylaldimine lanthanide nitrate complex with an unusual coordination mode.[8] This species, which self-assembles into a 2D coordination polymer, is obtained in situ in a one-step, metal-promoted condensation of salicylaldehyde with 1,4-butanediamine (putrescine, a biogenic amine). It displays infinite polymeric structure composed of networks of 10-coordinated lanthanum nodes linked by bridging unionized *N*,*N*′-bis(salicylidene)-1,4-butanediamine ligands that utilize only hydroxy oxygen atoms for coordination while the nitrogen atoms remain uncoordinated. To examine how the nature of the amine spacer can influence final supramolecular array we used a more rigid diamine precursor. This paper describes the definitive structural details correlated with spectral characterization of the new salicylaldimine lanthanide nitrate complexes containing *N*,*N*′-bis(salicylidene)-4-methyl-1,3-phenylenediamine (H_2L,

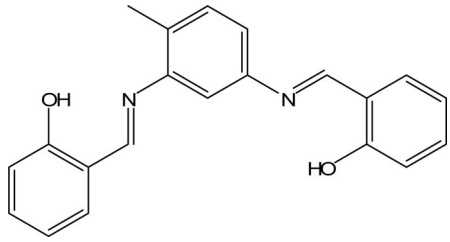

Scheme 1. *N*,*N*′-Bis(salicylidene)-4-methyl-1,3-phenylenediamine (H_2L).

[a] Faculty of Chemistry, Adam Mickiewicz University, Grunwaldzka 6, 60-780 Poznań, Poland
E-mail: wrp@amu.edu.pl
[b] Faculty of Chemistry, University of Wrocław, Joliot-Curie 14, 50-383 Wrocław, Poland

 © 2010 Wiley-VCH Verlag GmbH & Co. KGaA, Weinheim

Scheme 1) formed in the one-step [2+1] Schiff base condensation reaction between salicylaldehyde and 4-methyl-1,3-phenylenediamine in the presence of metal salts acting as template agents. They self-assemble into finite species and provide an example of monodentate exclusively oxygen-donor coordination behavior of a neutral salen-type ligand.

Results and Discussion

The new lanthanide salicylaldimine complexes of the formula $[Ln(H_2L)_3(NO_3)_3](H_2L)$, where Ln = La^{3+} (**1**), Nd^{3+} (**2**), Eu^{3+} (**3**), Gd^{3+} (**4**), Ho^{3+} (**5**), Er^{3+} (**6**), Tb^{3+} (**7**), or Yb^{3+} (**8**), and H_2L = *N*,*N*′-bis(salicylidene)-4-methyl-1,3-phenylenediamine, were formed in a self-assembly process involving the lanthanide template-induced one-step [2+1] Schiff base condensation reaction between salicylaldehyde and 4-methyl-1,3-phenylenediamine. Elemental analysis data of all the complexes are consistent with 1:4 lanthanide ion to H_2L ligand stoichiometry. The presence of three nitrate counterions in the complexes, which balance the charge of the metal cations, indicates that salicylaldimine ligands do not undergo deprotonation. However, single-crystal X-ray diffraction analysis of complexes **1**–**6** allowed us to establish the coordination arrangement around the metal cations and formulate these complexes as $[Ln(H_2L)_3(NO_3)_3](H_2L)$.

All the complexes are highly isostructural as might be seen from the very similar unit cell parameters in the same space group ($P2_1/n$) and almost identical positions of atoms in the crystal structures (Table 4).

Therefore, the discussion of one of the structures is equally valid for all the remaining cases (Figure 1).

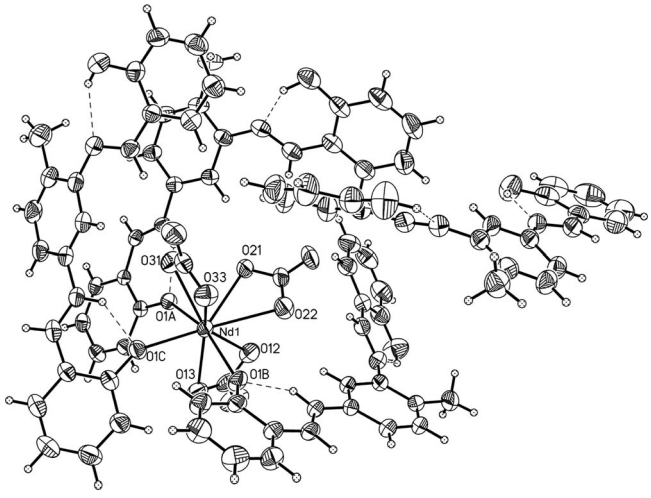

Figure 1. A perspective view of the unit-cell content of **2**. The ellipsoids are draw at the 50% probability level, hydrogen atoms are drawn as spheres of arbitrary radii, and hydrogen bonds are shown as dashed lines.

The Ln^{3+} ions are in a nine-coordinate environment with a coordination polyhedron that can be described as a tricapped trigonal prism. They are ligated by three bidentate nitrate anions and three oxygen atoms from three different undeprotonated H_2L ligand molecules (Figure 2).

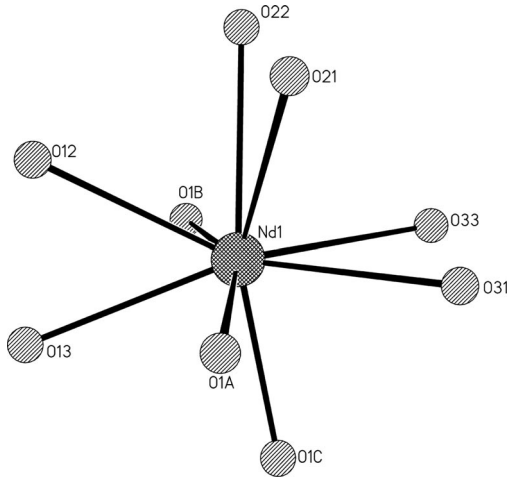

Figure 2. Coordination around the lanthanide ion.

The three neutral ligands are involved in coordination only through one of their two oxygen atoms. The other halves of these molecules are "free", not taking part in the coordination; additionally, there is one H_2L molecule in the crystal structure that is not bonded to the lanthanide ion at all. The positions of the hydrogen atoms were found from the Fourier maps, and it turned out that in the "coordinated" part of H_2L the hydrogen atoms are connected to N atoms, whereas in the "noncoordinated" parts they are connected to O atoms. All these N–H and O–H groups act as hydrogen-bond donors for intramolecular hydrogen bonds (cf. Table 1 for data for one exemplary structure).

Table 1. Hydrogen bond data for complex **2**.

D–H···A	D–H / Å	H···A / Å	D···A / Å	D–H···A / °
N8A–H8A···O1A	0.88(3)	1.90(3)	2.639(4)	141(3)
N8B–H8B···O1B	0.83(3)	1.98(4)	2.645(4)	137(3)
N8C–H8C···O1C	0.82(3)	2.01(3)	2.659(4)	136(3)
O19A–H19A···N16A	0.89(5)	1.81(5)	2.615(4)	148(5)
O19B–H19B···N16B	0.88(4)	1.87(5)	2.616(5)	142(4)
O19C–H19C···N16C	0.73(5)	2.03(5)	2.636(6)	141(5)
O1D–H1D···N8D	1.14(7)	1.61(7)	2.602(5)	142(5)
O19D–H19D···N16D	0.86(6)	1.87(6)	2.625(5)	146(6)

The differences in the bonding of the oxygen and nitrogen atoms influence of course the bond length patterns. The mean value of the C–O bond lengths for coordinating O atoms is 1.305(10) Å, while for noncoordinating O atoms it is 1.347(9) Å. Also, the lengths of the C=N bonds differ; the mean values are 1.302(6) and 1.279(6) Å for coordinated and uncoordinated parts, respectively.

The conformations of four independent ligand molecules differ; Table 2 lists the dihedral angles between the mean planes of three rings for one of the structures.

It seems that the uncoordinated ligand molecule is inserted in the "pocket" of the complex. This additional salicylaldimine molecule acts as a guest for the salicylaldimine complex host and stabilizes the overall self-assembled supramolecular network by weak C–H···π and π···π interactions (Figure 3).

 © 2010 Wiley-VCH Verlag GmbH & Co. KGaA, Weinheim

Table 2. Dihedral angles/° between the least-squares planes of phenyl rings (i: C1–C6, ii: C9–C15; iii: C18–C23) in the structure of **2**.

H_2L molecule	i/ii	i/iii	ii/iii
A	19.15(7)	32.37(14)	50.06(10)
B	6.37(14)	41.77(12)	35.54(13)
C	37.84(9)	24.34(12)	30.32(9)
D	12.27(17)	37.97(15)	28.38(19)

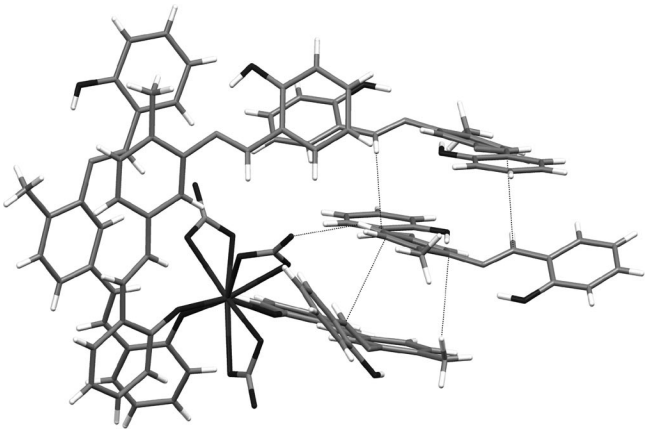

Figure 3. The weak interaction between the complex and inserted additional H_2L ligand molecule (cf. text).

Therefore, crystal structure analysis reveals the rare coordination pattern of the salicylaldimines in these complexes formed in situ from aldehyde and diamine precursors in self-assembled process. The potentially tetradentate heterodonor (N_2O_2) Schiff bases act as undeprotonated monodentate ligands: only one oxygen atom of each of the three ligands is involved in coordination. Neither the second oxygen atom nor any of the nitrogen atoms interact with the lanthanide ion; they are involved in intramolecular hydrogen bonds. The structural data are correlated with spectral characterization. The similarity between the spectroscopic data for the crystallographically characterized complexes (**1**–**6**) and for those for which no crystal data are available (**7** and **8**) allows us to assume analogous coordination mode in all the complexes. The ESI mass spectra provide strong evidence for the formation of the complexes with salicylaldimine H_2L as a product of the condensation reaction of two salicylaldehyde molecules with one 4-methyl-1,3-phenylenediamine molecule. The spectra exhibit peaks corresponding to the multiply charged species containing the metal ion coordinated to the three ligands and the peaks assignable to the free ligand. ^{1}H NMR spectroscopy of the diamagnetic lanthanum complex confirms the Schiff base condensation reaction and the presence of the undeprotonated neutral form of the ligands. Signals attributed to the imine protons are observed as singlets at δ = 9.01 and 9.03 ppm. The protons of the OH groups occur at δ = 13.14 and 13.29 ppm. The formation of the Schiff base in the complexes is also evidenced by strong IR absorption bands in the 1631–1597 cm^{-1} region, attributable to the C=N stretching mode and the absence of bands characteristic of carbonyl and amine groups of the starting materials. An important feature of the spectra of all the complexes is the occurrence of two absorption bands at 1632–1630 and 1602–1597 cm^{-1} associated with the presence of the two different C=N bonds. It is noted that the decrease in the C=N stretching frequency owing to the lowered double bond character is usually ascribed to the involvement of the nitrogen atom in the coordination moiety. However, this is not the case. The data gathered from both X-ray crystallography and spectroscopy reveal that in these complexes with a neutral form of the ligands the lower double bond character of the C=N bond is not caused by the involvement of the nitrogen atoms in the coordination but by proton transfer of the hydroxy groups to the nitrogen atoms. Thus, the higher frequency band may be assigned to the C=N groups involved in intramolecular hydrogen bonds, whereas the lower frequency band can be assigned to the protonated C=N groups. This behavior appears to be in accord with that from single-crystal structural analysis. The distances in the protonated C=N bonds are longer than the values found in the noncoordinated parts of the ligands involved in intraligand hydrogen bonds. The phenolic C–O bonds coordinated to the lanthanide ions are considerably shorter than the distances in the C–O bonds involved in intraligand hydrogen bonds and not in coordination. It is reflected by the presence of two IR absorption bands at 1286 and 1279 cm^{-1} associated with C–O stretching frequency. An absorption band at 502–501 cm^{-1} typical of metal–oxygen vibration provides the evidence of phenolic oxygen participation in the metal–ligand coordination. The two bands in the 3386–3355 and 3059–3028 cm^{-1} regions along with the weak band at 2859–2852 cm^{-1} indicate the presence of the six-membered rings formed by intramolecular hydrogen bonds between the hydroxy hydrogen and the nitrogen atoms of the azomethine groups. The IR spectra of all the lanthanide complexes show nitrate vibrations indicative of coordinated nitrate groups. The N–O stretching frequencies are observed as split bands in the 1466–1305 and 1778–1700 cm^{-1} regions and the band at 818–813 cm^{-1}. The profile and magnitude of band splitting associated with asymmetric nitrate vibrations, which is indicative of the interaction strength between the metal and the oxygen atoms of the nitrates, is consistent with the presence of the nitrate groups coordinating in a bidentate fashion.[8,9]

The photophysical properties of lanthanide complexes containing H_2L formed in situ in a one-step, metal-promoted condensation of aldehyde and diamine precursors were related to the behavior of this ligand in the free form obtained separately for comparison purposes.[10] Diffusion reflectance spectra of the H_2L and Ln–H_2L complexes, where Ln = La^{3+}, Nd^{3+}, Eu^{3+}, Gd^{3+}, Tb^{3+}, or Yb^{3+}, were recorded in the UV/Vis/NIR range and some of them are shown in Figure 4.

The UV/Vis region is dominated by an intense band belonging to the $\pi \rightarrow \pi^*$ transition of the Ar–OH chromophores and to the $n \rightarrow \pi^*$ transition of the imine groups. Because the expansion of the ligand band is significant, in the spectra of the compounds studied the most intense f–f

 © 2010 Wiley-VCH Verlag GmbH & Co. KGaA, Weinheim

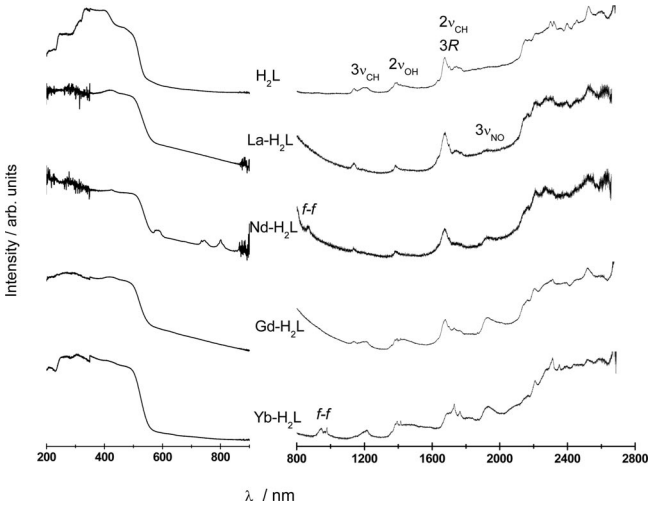

Figure 4. Diffusion reflectance spectra of the H_2L and Ln–H_2L complexes.

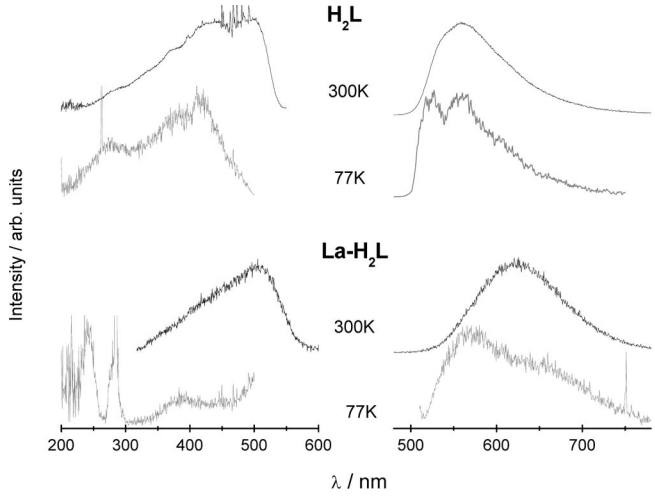

Figure 6. Excitation ($\lambda_{em} \approx 550$ nm) and emission ($\lambda_{exc} \approx 400$ nm) spectra of the H_2L and La–H_2L complex at 300 and 77 K.

transitions can be seen for the Nd^{3+} complex only. The NIR spectra display peaks that belong to overtones and/or their combination bands of higher energy vibrations of the ligand in complexes.[11] The only f–f transitions that do not overlap with vibration bands were found in the spectra of the Nd^{3+} ($^4I_{9/2} \rightarrow {}^4F_{3/2}$ transition) and Yb^{3+} ($^2F_{7/2} \rightarrow {}^2F_{5/2}$ transition) complexes. The peak located between 1900 and 2000 nm is observed in the spectra of the complexes only. Therefore, it was assigned as the second overtone of ν_{NO} of the nitrate anions. The reflectance spectrum of the Yb^{3+}–H_2L complex shown in Figure 5 was used for the energy level determination of the $^2F_{7/2} \rightarrow {}^2F_{5/2}$ transition.

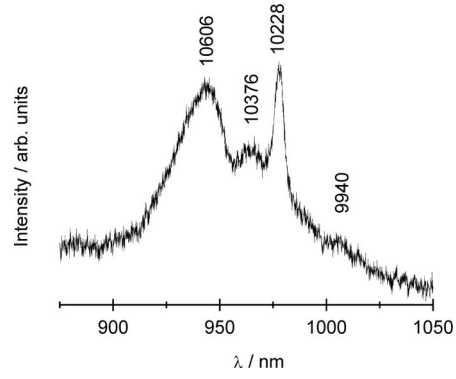

Figure 5. Reflectance spectrum of the $^2F_{7/2} \rightarrow {}^2F_{5/2}$ transition in the Yb–H_2L complex.

The position of the $^2F_{5/2}(0)$ level equal to 10228 cm^{-1} is redshifted in comparison to those previously found by us for pentaaza macrocyclic[12] and carboxylic[13] ytterbium complexes. The splitting of the $^2F_{5/2}$ manifold by the ligand field in the current compound was determined as 0, 148, and 378 cm^{-1}.

The excitation and emission spectra of the H_2L ligand and its La^{3+} complex were measured at room temperature and at 77 K and are shown in Figure 6.

All complex samples excited by the ligand absorption bands at 245 and 400 nm, also those that have f electron levels (Nd^{3+}, Eu^{3+}, and Tb^{3+}) at similar energies as those of the ligand triplet state, exhibit a weak ligand-centered emission in the range 500–800 nm. Their emission spectra recorded at 300 and 77 K are presented in Figure 7.

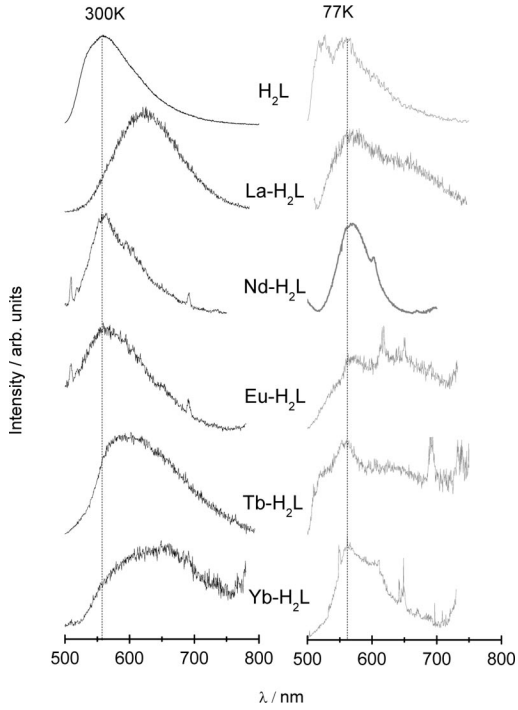

Figure 7. Emission spectra ($\lambda_{exc} \approx 400$ nm) of the H_2L and Ln–H_2L complexes (some minor peaks are characteristic for the Xe lamp).

It should be noted that Nd^{3+} and Yb^{3+} complexes have been also measured through direct excitation into the $^4F_{3/2}$ and $^2F_{5/2}$ states, but attempts to record their characteristic lanthanide emission spectra failed. The emission spectra shown in Figure 7 indicate that the triplet-state energies at room temperature undergo different changes depending on

 © 2010 Wiley-VCH Verlag GmbH & Co. KGaA, Weinheim

the lanthanide ion. This can be related to the matching of energy levels of the Ln^{3+} ions and the H_2L ligand as well as to the change in the effective charge of the metal cation and its size. Though ligand-centered phosphorescence is weaker in the spectra recorded at 77 K than at room temperature, the maximum of the emission band is placed nearly at the same wavenumber for all the Ln–H_2L complexes.

The time decay characteristics of the triplet state have been also performed. The samples of the ligand and the Eu^{3+} and Tb^{3+} complexes were excited by a xenon flash-lamp at 77 K, whereas the excitation of the Nd^{3+} and Yb^{3+} complexes was provided by the OPO pumped by a Nd:YAG laser. For the latter samples, the emission decay curves were detected only for the Yb^{3+} compound. The results are presented in Table 3.

Table 3. Emission lifetimes (τ) of H_2L as free ligand and in its complexes with Tb^{3+} and Yb^{3+} ions.

Compounds	λ_{exc} / nm	λ_{em} / nm	τ / ns
H_2L	400	527	3
Eu–H_2L	380	617	1.4
Tb–H_2L	380	545	1.8
Yb–H_2L	476	990	3200
Yb–H_2L	930	990	3700

The decrease in emission lifetimes of H_2L in the Eu^{3+} and Tb^{3+} complexes compared to the free H_2L ligand is caused by significant matching of the electronic levels of metal ions and the triplet state of the ligand. The luminescence lifetimes of the Yb^{3+} ion (excited into triplet and $^2F_{5/2}$ states) indicate that energy transfer between electronic levels of the ligand and the Yb^{3+} ion is inefficient. Thus, the photophysical processes that occur in the compounds studied are schematically presented in Figure 8.

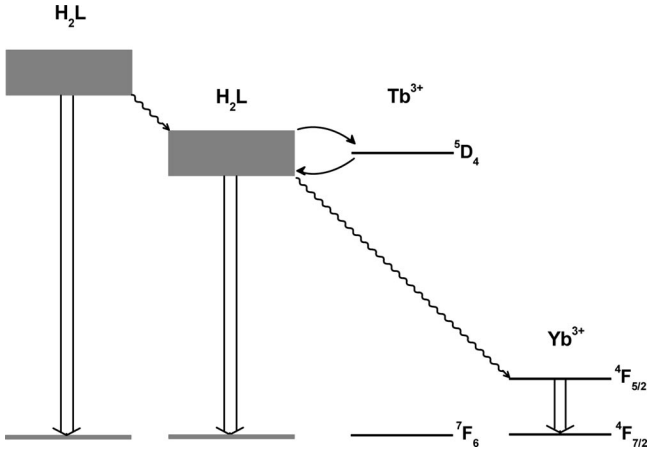

Figure 8. Scheme of photophysical processes in H_2L and its complexes with Tb^{3+} and Yb^{3+} ions.

Excitation of the ligand-centered absorption bands produces ligand-centered emissions, which implies that the ligand-to-metal energy transfer is unsuccessful.

Conclusions

Our results involving the synthesis and identification of the new lanthanide salicylaldimine complexes extend a relatively scarce number of structurally defined salen-type lanthanide complexes and provide an example of multilevel inorganic self-organization. In these species with lanthanide ions displaying the nine-coordinate distorted tricapped trigonal prism geometry, the nitrates function as bidentate chelators occupying six coordination sites and leaving the remaining sites available for salicylaldimine ligands formed in situ from aldehyde and diamine precursors in the metal-template process. The lanthanide ions serve as templating and assembling centers for the construction of the salicylaldimine lanthanide complexes, which act as hosts for the additional salicylaldimine molecule guest stabilizing the overall self-assembled supramolecular network. The neutral monodentate exclusively O-donor-type coordination found in these lanthanide complexes is in marked contrast to the dianionic tetradentate N_2O_2 donor set arrangement typically observed in most salen-type coordination compounds. Structural analysis correlated with spectroscopic studies of this rare coordination pattern reveals that the effects of nitrogen protonation and coordination of the metal ion through oxygen only on bond lengths are remarkably similar to those caused be the removal of protons by ionization and coordination of all oxygen and nitrogen atoms. Therefore, the coordination mode in salen-type complexes might have been incorrectly inferred from spectroscopic analysis alone. The characterization of these salicylaldimine lanthanide complexes by both X-ray crystallography and spectroscopic methods may be useful in guiding and confirming interpretations concerning the coordination modes of other related complexes for which no crystal data are available and may provide valuable information for their structural studies.

Experimental Section

Materials: Lantanum(III), neodymium(III), europium(III), gadolinium(III), terbium(III), holmium(III), erbium(III), and ytterbium(III) nitrates, salicylaldehyde, and 4-methyl-1,3-phenylenediamine were obtained from the Aldrich Chemical Company. 4-Methyl-1,3-phenylenediamine was purified by recrystallization from *n*-heptane.

Physical Measurements: The complexes were characterized by using microanalyses (CHN), IR, UV/Vis–NIR, and ^1H NMR spectroscopy, ESI-MS, and single-crystal X-ray diffraction analysis. IR spectra were recorded by using KBr pellets in the range 4000–400 cm^{-1} with a Bruker IFS 66v/S spectrophotometer. Mass spectra were performed by using electrospray ionization (ESI) techniques. Electrospray mass spectra were determined in ethanol by using Waters Micromass ZQ spectrometer. The sample was run in the positive-ion mode. The concentration of the compound was about 10^{-4} mol dm^{-3}. Sample solution was introduced into the mass spectrometer source with a syringe pump with a flow rate of 40 μL min^{-1}, a capillary voltage of +3 kV, and a desolvation temperature of 300 °C. The source temperature was 120 °C. The cone voltage (V_c) was set to 30 V to allow transmission of ions without

 © 2010 Wiley-VCH Verlag GmbH & Co. KGaA, Weinheim

fragmentation processes. Scanning was performed from *m*/*z* = 100 to 1000 in 6 s, and 10 scans were summed to obtain the final spectrum. ^{1}H NMR spectra were recorded in [D$_6$]DMSO with a Varian Gemini 300 spectrometer with chemical shift (ppm) values reported relative to TMS as an internal reference. Electronic absorption spectra were measured with a JASCO V-550 spectrophotometer in ethanol. Microanalyses (CHN) were obtained by using a Perkin–Elmer 2400 CHN microanalyzer. Diffusion reflectance spectra of the H_2L and Ln–H_2L complexes (where Ln = La^{3+}, Nd^{3+}, Eu^{3+}, Gd^{3+}, Tb^{3+}, and Yb^{3+}) were recorded in the UV/Vis and NIR region with a Cary 5 UV/Vis–NIR spectrophotometer, whereas excitation and emission spectra as well as luminescence decay curves were measured with an FLS920 Edinburgh Instruments Ltd at room temperature and at 77 K. Upon excitation of the samples of ligand and Eu^{3+} and Tb^{3+} complexes at ca. 400 nm, the luminescence decay curves were detected with the monitored emission in the range 500–600 nm at 77 K by using an F900 high-power xenon flashlamp. The samples of neodymium and ytterbium complexes were also excited resonantly into $^4F_{3/2}$ (870 nm) and $^2F_{5/2}$ (930 nm) levels and at 476 nm with a Continuum Surelite I Optical Parametric Oscillator pumped by a third harmonic of an Nd:YAG laser with monitored emission at 1064 and 990 nm, respectively. These measurements were taken at room temperature, and the luminescence decay curves were detected on a device equipped with a Hamamatsu photomultiplier and a Tektronix TDS-3052 digital oscilloscope. All luminescence decay lifetimes were obtained by fitting the decay curves to a single exponential function.

[La(H$_2$L)$_3$(NO$_3$)$_3$](H$_2$L) (1): To a mixture of lantanum(III) nitrate (43 mg, 0.1 mmol) in ethanol (10 mL) and salicylaldehyde (92 mg, 0.8 mmol) in ethanol (10 mL) was added 4-methyl-1,3-phenylenediamine (36 mg, 0.3 mmol) in ethanol (10 mL) dropwise with stirring. The reaction was carried out for 24 h at room temperature. The solution volume was then reduced to 5 mL by roto-evaporation, and orange single crystals suitable for X-ray diffraction analysis were formed by slow evaporation of the solvent. Yield: 61%. $C_{84}H_{72}LaN_{11}O_{17}\cdot H_2O$ (1663.45): calcd. C 60.61, H 4.48, N 9.26; found C 59.03, H 4.39, N 9.05. IR (KBr): $\tilde{\nu}$ = 3375, 3056 (ν_{OH}), 2854 ($\nu_{OH\cdots N}$), 1630, 1597 ($\nu_{C=N}$), 1486, 1189, 1150, 1037, 1000, 756 ($\nu_{C=C}$), 1286, 1279 (ν_{C-O}), 501 (ν_{La-O}), 1731, 1700, 1454–1305, 1384, 818 (ν_{NO}) cm^{-1}. ^{1}H NMR (300 MHz, [D$_6$]DMSO, Me$_4$Si): δ = 2.36 (s, 3 H, phen-CH$_3$), 6.98 (d, *J* = 7.51 Hz, 2 H, aryl), 7.03 (d, *J* = 7.51 Hz, 2 H, aryl), 7.31 (d, *J* = 7.88 Hz, 1 H, phen), 7.31 (s, 1 H, phen), 7.43 (d, *J* = 7.69 Hz, 2 H, aryl), 7.65 (d, *J* = 7.88 Hz, 1 H, phen), 7.69, 7.68 (2 d, *J* = 7.69 Hz, 2 H), 9.01, 9.03 (2 s, 1 H, HC=N), 9.05, 9.06 (2 s, 1 H, HC=N), 13.14, 13.29 (2 s, 2 H, 2 OH) ppm. UV/Vis (EtOH): λ (ε, M^{-1} cm^{-1}) = 211 (115000), 248 (32400), 271 (62600), 306 (44000), 348 (62800) nm. MS (ESI, MeOH): *m*/*z* = 376 [La(C$_{21}$H$_{18}$N$_2$O$_2$)$_3$]$^{3+}$, 331 [C$_{21}$H$_{18}$N$_2$O$_2$ + H]$^+$.

[Nd(H$_2$L)$_3$(NO$_3$)$_3$](H$_2$L) (2): To a mixture of neodymium(III) nitrate (44 mg, 0.1 mmol) in ethanol (10 mL) and salicylaldehyde (69 mg, 0.6 mmol) in ethanol (10 mL) was added 4-methyl-1,3-phenylenediamine (24 mg, 0.2 mmol) in ethanol (10 mL) dropwise with stirring. The reaction was carried out for 24 h at room temperature. The solution volume was then reduced to 5 mL by roto-evaporation, and deep-red single crystals suitable for X-ray diffraction analysis were formed by slow evaporation of the solvent. Yield: 63%. $C_{84}H_{72}N_{11}NdO_{17}\cdot H_2O$ (1669.79): calcd. C 60.42, H 4.47, N 9.23; found C 57.38, H 4.23, N 8.86. IR (KBr): $\tilde{\nu}$ = 3386, 3056 (ν_{OH}), 2854 ($\nu_{OH\cdots N}$), 1630, 1599 ($\nu_{C=N}$), 1486, 1188, 1142, 1039, 1000, 756 ($\nu_{C=C}$), 1286, 1279 (ν_{C-O}), 501 (ν_{Nd-O}), 1731, 1701, 1405–1368, 1384, 812 (ν_{NO}) cm^{-1}. UV/Vis (EtOH): λ (ε, M^{-1} cm^{-1}) = 215 (345600), 248 (161800), 267 (197800), 292 (115000), 346 (171000) nm. MS (ESI, MeOH): *m*/*z* = 377 [Nd(C$_{21}$H$_{18}$N$_2$O$_2$)$_3$]$^{3+}$, 331 [C$_{21}$H$_{18}$N$_2$O$_2$ + H]$^+$.

[Eu(H$_2$L)$_3$(NO$_3$)$_3$](H$_2$L) (3): To a mixture of europium(III) nitrate (45 mg, 0.1 mmol) in ethanol (10 mL) and salicylaldehyde (69 mg, 0.6 mmol) in ethanol (10 mL) was added 4-methyl-1,3-phenylenediamine (24 mg, 0.3 mmol) in ethanol (10 mL) dropwise with stirring. The reaction was carried out for 24 h at room temperature. The solution volume was then reduced to 5 mL by roto-evaporation, and orange single crystals suitable for X-ray diffraction analysis were formed by slow evaporation of the solvent. Yield: 62%. $C_{84}H_{72}EuN_{11}O_{17}\cdot 2H_2O$ (1665.53): calcd. C 59.50, H 4.52, N 9.09; found C 58.14, H 4.39, N 9.27. IR (KBr): $\tilde{\nu}$ = 3375, 3059 (ν_{OH}), 2859 ($\nu_{OH\cdots N}$), 1632, 1602 ($\nu_{C=N}$), 1486, 1188, 1142, 1037, 1002, 756 ($\nu_{C=C}$), 1286, 1279 (ν_{C-O}), 501 (ν_{Eu-O}), 1733, 1718, 1460–1370, 1384, 814 (ν_{NO}) cm^{-1}. UV/Vis (EtOH): λ (ε, M^{-1} cm^{-1}) = 211 (192400), 249 (59400), 270 (99000), 294 (66600), 348 (94000) nm. MS (ESI, MeOH): *m*/*z* = 381 [Eu(C$_{21}$H$_{18}$N$_2$O$_2$)$_3$]$^{3+}$, 331 [C$_{21}$H$_{18}$N$_2$O$_2$ + H]$^+$.

[Gd(H$_2$L)$_3$(NO$_3$)$_3$](H$_2$L) (4): To a mixture of gadolinium(III) nitrate (45 mg, 0.1 mmol) in ethanol (10 mL) and salicylaldehyde (92 mg, 0.8 mmol) in ethanol (10 mL) was added 4-methyl-1,3-phenylenediamine (36 mg, 0.3 mmol) in ethanol (10 mL) dropwise with stirring. The reaction was carried out for 24 h at room temperature. The solution volume was then reduced to 5 mL by roto-evaporation, and dark-orange single crystals suitable for X-ray diffraction analysis were formed by slow evaporation of the solvent. Yield: 62%. $C_{84}H_{72}GdN_{11}O_{17}\cdot 3H_2O$ (1718.83): calcd. C 58.70, H 4.57, N 8.96; found C 57.07, H 4.39, N 9.22. IR (KBr): $\tilde{\nu}$ = 3372, 3057 (ν_{OH}), 2854 ($\nu_{OH\cdots N}$), 1631, 1599 ($\nu_{C=N}$), 1487, 1188, 1143, 1040, 1000, 756 ($\nu_{C=C}$), 1286, 1279 (ν_{C-O}), 501 (ν_{Gd-O}), 1742, 1732, 1702, 1464–1323, 1384, 812 (ν_{NO}) cm^{-1}. UV/Vis (EtOH): λ (ε, M^{-1} cm^{-1}) = 211 (141400), 253 (44200), 273 (73200), 306 (54200), 348 (65800) nm. MS (ESI, MeOH): *m*/*z* = 411 [Gd(C$_{21}$H$_{18}$N$_2$O$_2$)$_3$-(H$_2$O)$_3$(CH$_3$OH)]$^{3+}$, 395 [Gd(C$_{21}$H$_{18}$N$_2$O$_2$)$_3$(H$_2$O)$_2$]$^{3+}$, 331 [C$_{21}$H$_{18}$N$_2$O$_2$ + H]$^+$.

[Ho(H$_2$L)$_3$(NO$_3$)$_3$](H$_2$L) (5): To a mixture of holmium(III) nitrate (46 mg, 0.1 mmol) in ethanol (10 mL) and salicylaldehyde (69 mg, 0.6 mmol) in ethanol (10 mL) was added 4-methyl-1,3-phenylenediamine (24 mg, 0.2 mmol) in ethanol (10 mL) dropwise with stirring. The reaction was carried out for 24 h at room temperature. The solution volume was then reduced to 5 mL by roto-evaporation, and orange single crystals suitable for X-ray diffraction analysis were formed by slow evaporation of the solvent. Yield: 62%. $C_{84}H_{72}HoN_{11}O_{17}$ (1672.44): calcd. C 60.32, H 4.34, N 9.21; found C 59.85, H 4.24, N 9.25. IR (KBr): $\tilde{\nu}$ = 3368, 3057 (ν_{OH}), 2854 ($\nu_{OH\cdots N}$), 1631, 1598 ($\nu_{C=N}$), 1488, 1189, 1144, 1042, 1000, 756 ($\nu_{C=C}$), 1286, 1279 (ν_{C-O}), 502 (ν_{Ho-O}), 1774, 1734, 1465–1327, 1384, 813 (ν_{NO}) cm^{-1}. UV/Vis (EtOH): λ (ε, M^{-1} cm^{-1}) = 215 (331000), 249 (129400), 270 (186800), 294 (108600), 347 (154600) nm. MS (ESI, MeOH): *m*/*z* = 385 [Ho(C$_{21}$H$_{18}$N$_2$O$_2$)$_3$]$^{3+}$, 331 [C$_{21}$H$_{18}$N$_2$O$_2$ + H]$^+$.

[Er(H$_2$L)$_3$(NO$_3$)$_3$](H$_2$L) (6): To a mixture of lantanum(III) nitrate (46 mg, 0.1 mmol) in ethanol (10 mL) and salicylaldehyde (69 mg, 0.6 mmol) in ethanol (10 mL) was added 4-methyl-1,3-phenylenediamine (24 mg, 0.2 mmol) in ethanol (10 mL) dropwise with stirring. The reaction was carried out for 24 h at room temperature. The solution volume was then reduced to 5 mL by roto-evaporation, and orange single crystals suitable for X-ray diffraction analysis were formed by slow evaporation of the solvent. Yield: 63%. $C_{84}H_{72}ErN_{11}O_{17}$ (1672.44): calcd. C 60.24, H 4.33, N 9.20; found C 59.79, H 4.20, N 9.17. IR (KBr): $\tilde{\nu}$ = 3366, 3058 (ν_{OH}), 2856 ($\nu_{OH\cdots N}$), 1631, 1598 ($\nu_{C=N}$), 1488, 1189, 1144, 1042, 1000, 756

 © 2010 Wiley-VCH Verlag GmbH & Co. KGaA, Weinheim

($\nu_{C=C}$), 1286, 1279 (ν_{C-O}), 502 (ν_{Er-O}), 1775, 1734, 1466–1353, 1384, 813 (ν_{NO}) cm^{-1}. UV/Vis (EtOH): λ (ε, $M^{-1}cm^{-1}$) = 211 (101600), 246 (25400), 271 (54000), 306 (38800), 348 (54600) nm. MS (ESI, MeOH): *m/z* = 385 $[Er(C_{21}H_{18}N_2O_2)_3]^{3+}$, 331 $[C_{21}H_{18}N_2O_2 + H]^+$.

$[Tb(H_2L)_3(NO_3)_3](H_2L)$ (7): To a mixture of lantanum(III) nitrate (45 mg, 0.1 mmol) in ethanol (10 mL) and salicylaldehyde (69 mg, 0.6 mmol) in ethanol (10 mL) was added 4-methyl-1,3-phenylenediamine (24 mg, 0.2 mmol) in ethanol (10 mL) dropwise with stirring. The reaction was carried out for 24 h at room temperature. The solution volume was then reduced to 5 mL by roto-evaporation, and a red precipitate was formed by slow evaporation of the solvent. Yield: 61%. $C_{84}H_{72}N_{11}O_{17}Tb{\cdot}H_2O$ (1683.47): calcd. C 59.89, H 4.43, N 9.15; found C 59.95, H 4.92, N 9.12. IR (KBr): $\tilde{\nu}$ = 3380, 3056 (ν_{OH}), 2854 ($\nu_{OH\cdots N}$), 1630, 1597 ($\nu_{C=N}$), 1487, 1189, 1143, 1040, 1000, 757 ($\nu_{C=C}$), 1280 (ν_{C-O}), 502 (ν_{Tb-O}), 1742, 1733, 1704, 1418–1358, 1384, 812 (ν_{NO}) cm^{-1}. UV/Vis (EtOH): λ (ε, $M^{-1}cm^{-1}$) = 211 (142400), 251 (45200), 271 (74300), 305 (56300), 347 (64500) nm. MS (ESI, MeOH): *m/z* = 394 $[Tb(C_{21}H_{18}N_2O_2)_3(CH_3OH)]^{3+}$, 331 $[C_{21}H_{18}N_2O_2 + H]^+$.

$[Yb(H_2L)_3(NO_3)_3](H_2L)$ (8): To a mixture of ytterbium(III) nitrate (47 mg, 0.1 mmol) in ethanol (10 mL) and salicylaldehyde (69 mg, 0.6 mmol) in ethanol (10 mL) was added 4-methyl-1,3-phenylenediamine (24 mg, 0.2 mmol) in ethanol (10 mL) dropwise with stirring. The reaction was carried out for 24 h at room temperature. The solution volume was then reduced to 5 mL by roto-evaporation, and an orange precipitate was formed by slow evaporation of the solvent. Yield: 64%. $C_{84}H_{72}N_{11}O_{17}Yb$ (1680.45): calcd. C 60.03, H 4.32, N 9.17; found C 58.64, H 4.12, N 8.75. IR (KBr): $\tilde{\nu}$ = 3365, 3028 (ν_{OH}), 2852 ($\nu_{OH\cdots N}$), 1630, 1597 ($\nu_{C=N}$), 1488, 1189, 1144, 1043, 999, 757 ($\nu_{C=C}$), 1286, 1279 (ν_{C-O}), 502 (ν_{Yb-O}), 1778, 1735, 1465–1370, 1384, 813 (ν_{NO}) cm^{-1}. UV/Vis (EtOH): λ (ε, $M^{-1}cm^{-1}$) = 211 (138200), 249 (39200), 271 (81000), 306 (58200), 348 (82200) nm. MS (ESI, MeOH): *m/z* = 394 $[Yb(C_{21}H_{18}N_2O_2)_3(H_2O)]^{3+}$, 331 $[C_{21}H_{18}N_2O_2 + H]^+$.

Crystal Structure Determination: Diffraction data were collected at room temperature by the ω-scan technique with a KUMA-KM4CCD diffractometer[14] with graphite-monochromated Mo-K_α radiation (λ = 0.71073 Å). The data were corrected for Lorentz-polarization effects as well as for absorption. Accurate unit-cell parameters were determined by a least-squares fit of 16038 (for **1**) 29976 (for **2**), 2547 (for **3**), 17192 (for **4**), 4758 (for **5**), and 2734 (for **6**) reflections of highest intensity, chosen from the whole experiment. The structures were solved with SIR-92[15] and refined with the full-matrix least-squares procedure on F^2 by SHELXL97.[16] Scattering factors incorporated in SHELXL97 were used. All non-hydrogen atoms were refined anisotropically. In the structures of **2** and **4**, which are of the best quality, positions of the hydrogen atoms involved in intramolecular hydrogen bonds (N–H or O–H groups) were located in subsequent difference Fourier maps and their positional and isotropic displacement parameters were refined. Due to the isostructural nature of all the structures, the same positions of the hydrogen atoms (bonded to nitrogen or oxygen atoms) were assumed in the remaining four structures. All the other hydrogen atoms were placed geometrically, in idealized positions, and refined as rigid groups, U_{iso} of hydrogen atoms were set as 1.2 (1.3 for CH_3 groups) times U_{eq} of the appropriate carrier atom. Relevant crystal data are listed in Table 4, together with refinement details.

CCDC-751632 (for **1**), -751633 (for **2**), -751634 (for **3**), -751635 (for **4**), -751636 (for **5**), and -751637 (for **6**) contain the supplementary crystallographic data for this paper. These data can be obtained free of charge from the Cambridge Crystallographic Data Centre via www: www.ccdc.cam.ac.uk/data_request/cif.

Table 4. Crystal data, data collection, and structure refinement for complexes **1**–**6**.

Compound	**1**	**2**	**3**	**4**	**5**	**6**
Formula	$[La(NO_3)_3(C_{21}H_{18}N_2O_2)_3]{\cdot}(C_{21}H_{18}N_2O_2)$	$[Nd(NO_3)_3(C_{21}H_{18}N_2O_2)_3]{\cdot}(C_{21}H_{18}N_2O_2)$	$[Eu(NO_3)_3(C_{21}H_{18}N_2O_2)_3]{\cdot}(C_{21}H_{18}N_2O_2)$	$[Gd(NO_3)_3(C_{21}H_{18}N_2O_2)_3]{\cdot}(C_{21}H_{18}N_2O_2)$	$[Ho(NO_3)_3(C_{21}H_{18}N_2O_2)_3]{\cdot}(C_{21}H_{18}N_2O_2)$	$[Er(NO_3)_3(C_{21}H_{18}N_2O_2)_3]{\cdot}(C_{21}H_{18}N_2O_2)$
Formula weight	1646.46	1651.77	1659.49	1664.78	1672.46	1674.79
Crystal system	monoclinic	monoclinic	monoclinic	monoclinic	monoclinic	monoclinic
Space group	$P2_1/c$ (no. 14)	$P2_1/c$ (no. 14)	$P2_1/c$ (no. 14)	$P2_1/c$ (no. 14)	$P2_1/c$ (no. 14)	$P2_1/c$ (no. 14)
a / Å	17.6053(9)	17.5293(6)	17.4009(13)	17.4345(7)	17.4752(8)	17.3867(17)
b / Å	15.2434(8)	15.2329(8)	15.244(2)	15.2247(6)	15.2401(11)	15.2569(17)
c / Å	28.9050(16)	28.8812(8)	28.920(3)	28.8701(8)	28.910(2)	28.915(3)
β / °	95.714(4)	95.194(3)	94.504(7)	94.719(3)	94.867(5)	94.444(7)
V / Å^3	7718.5(7)	7680.3(5)	7647.6(14)	7637.2(5)	7671.7(8)	7647.1(14)
Z	4	4	4	4	4	4
D_x / g cm^{-3}	1.42	1.43	1.44	1.45	1.45	1.46
F(000)	3384	3396	3408	3412	3424	3428
μ / mm^{-1}	0.63	0.75	0.90	0.95	1.11	1.18
Θ range / °	1.95–25.00	1.87–28.22	5.40–25.00	2.21–27.95	1.87–25.00	2.21–25.00
Reflections:						
Collected	81499	146069	9552	44765	31880	64778
Unique (R_{int})	13591 (0.107)	17670 (0.067)	6549 (0.25)	16568 (0.030)	13384 (0.099)	13465 (0.414)
with $I > 2\sigma(I)$	7491	8888	998	10393	5089	2164
Number of parameters	1022	1054	1018	1054	1018	1018
$R(F)$ [$I > 2\sigma(I)$]	0.081	0.036	0.060	0.035	0.070	0.033
$wR(F^2)$ [$I > 2\sigma(I)$]	0.112	0.072	0.051	0.059	0.140	0.031
$R(F)$ [all data]	0.152	0.111	0.390	0.085	0.197	0.308
$wR(F^2)$ [all data]	0.131	0.104	0.084	0.086	0.171	0.063
Goodness of fit	1.381	1.053	0.594	1.14	0.95	0.39
Max./min. $\Delta\rho$ / e Å^{-3}	1.66/–0.77	1.62/–0.44	0.51/–0.31	2.14/–0.84	1.09/–0.87	0.34/–0.42

 © 2010 Wiley-VCH Verlag GmbH & Co. KGaA, Weinheim

Acknowledgments

This work was supported by the Ministry of Science and Higher Education (grant NN204031733).

[1] P. A. Vigato, S. Tamburini, *Coord. Chem. Rev.* **2004**, *248*, 1717–2128.

[2] a) H. Jacobsen, L. Cavallo, *Chem. Eur. J.* **2001**, *7*, 800–807; b) P. G. Cozzi, *Chem. Soc. Rev.* **2004**, *33*, 410–421; c) E. Jacobsen, *Acc. Chem. Res.* **2000**, *33*, 421–431; d) T. Katsuki, *Chem. Soc. Rev.* **2004**, *33*, 437–444; e) . S. Venkataramanan, G. Kuppuraj, S. Rajagopal, *Coord. Chem. Rev.* **2005**, *249*, 1249–1268; f) F. Rajabi, *Tetrahedron Lett.* **2009**, *50*, 395–397; g) A. W. Kleij, *Eur. J. Inorg. Chem.* **2009**, 193–205.

[3] a) K. Binnemans, K. Lodewyckx, T. Cardinaels, T. N. Parac-Vogt, C. Bourgogne, D. Guillon, B. Donnio, *Eur. J. Inorg. Chem.* **2006**, *1*, 150–157; b) D. Cunningham, P. McArdle, M. Mitchell, N. N. Chonchubhair, M. O'Gara, *Inorg. Chem.* **2000**, *39*, 1639–1649; c) W. Huang, H.-B. Zhu, S.-H. Gou, *Coord. Chem. Rev.* **2006**, *250*, 414–423; d) R. Gheorghe, M. Andruh, J.-P. Costes, B. Donnadieu, *Chem. Commun.* **2003**, 2778–2779; e) Z. Li, C. Jablonski, *Inorg. Chem.* **2000**, *39*, 2456–2461; f) W.-K. Lo, W.-K. Wong, J. Guo, W.-Y. Wong, K.-F. Li, K.-W. Cheah, *Inorg. Chim. Acta* **2004**, *357*, 4510–4521; g) J. He, Y.-G. Yin, X.-C. Huang, D. Li, *Inorg. Chem. Commun.* **2006**, *9*, 205–207; h) L. Rigamonti, F. Demartin, A. Forni, S. Righetto, A. Pasini, *Inorg. Chem.* **2006**, *45*, 10976–10989; i) M. Yuan, F. Zhao, W. Zhang, Z.-M. Wang, S. Gao, *Inorg. Chem.* **2007**, *46*, 11235–11242; j) L. Mishra, R. Prajapati, K. Kimura, S. Kobayashi, *Inorg. Chem. Commun.* **2007**, *10*, 1040–1044; k) Z.-H. Ni, L.-F. Zhang, V. Tangoulis, W. Wernsdorfer, A.-L. Cui, O. Sato, H.-Z. Kou, *Inorg. Chem.* **2007**, *46*, 6029–6037.

[4] a) D. P. Riley, *Chem. Rev.* **1999**, *99*, 2573–2587; b) J. Ziegler, T. Schuerle, L. Pasierb, C. Kelly, A. Elamin, K. A. Cole, D. W. Wright, *Inorg. Chem.* **2000**, *39*, 3731–3733; c) H. Eshtiagh-Hosseini, M. R. Housaindakht, S. A. Beyramabadi, S. Beheshti, A. A. Esmaeili, M. J. Khoshkholgh, A. Morsali, *Spectrochim. Acta Part A* **2008**, *71*, 1341–1347; d) M. A. Neelakantan, F. Rusalraj, J. Dharmaraja, S. Johnsonraja, T. Jeyakumar, M. Sankaranarayana Pillai, *Spectrochim. Acta Part A* **2008**, *71*, 1599–1609; e) A. Puglisi, G. Tabbi, G. Vecchio, *J. Inorg. Biochem.* **2004**, *98*, 969–976; f) V. Daier, H. Biava, C. Palopoli, S. Shova, J.-P. Tuchagues, S. Signorella, *J. Inorg. Biochem.* **2004**, *98*, 1806–1817; g) F. Cisnetti, G. Pelosi, C. Policar, *Inorg. Chim. Acta* **2007**, *360*, 557–562.

[5] a) L. Benisvy, R. Kannappan, Y.-F. Song, S. Milikisyants, M. Huber, I. Mutikainen, V. Turpeinen, P. Gamez, L. Bernasconi, E. J. Baerends, F. Hartl, J. Reedijk, *Eur. J. Inorg. Chem.* **2007**, 637–642; b) J. He, Y.-G. Yin, X.-C. Huang, D. Li, *Inorg. Chem. Commun.* **2006**, *9*, 205–207; c) N. Chantarasini, V. Ruangpornvisuti, N. Munangsin, H. Detsen, T. Mananunsp, C. Batiya, N. Chaichit, *J. Mol. Struct.* **2004**, *701*, 93–103; d) R. C. Howell, K. V. N. Spence, I. A. Kahwa, D. J. Williams, *J. Chem. Soc., Dalton Trans.* **1998**, 2727–2734; e) Q. Liu, C. Meermann, H. W. Görlitzer, O. Runte, E. Herdtweck, P. Sirsch, K. W. Törnroos, P. Anwander, *Dalton Trans.* **2008**, 6170–6178.

[6] a) M. P. Hogerheide, J. Boersma, G. van Koten, *Coord. Chem. Rev.* **1996**, *155*, 87–126; b) A. Terzis, D. Mentzafos, H. A. Tajmir-Riahi, *Inorg. Chim. Acta* **1984**, *84*, 187–193; c) Y.-P. Cai, H.-Z. Ma, B.-S. Kang, C.-Y. Su, W. Zhang, J. Sun, Y.-L. Xiong, *J. Organomet. Chem.* **2001**, *628*, 99–106; d) X. Yang, B. P. Hahn, R. A. Jones, W.-K. Wong, K. J. Stevenson, *Inorg. Chem.* **2007**, *46*, 7050–7054; e) X. Yang, R. A. Jones, W.-K. Wong, *Chem. Commun.* **2008**, *28*, 3266–3268; f) X. Yang, R. A. Jones, *J. Am. Chem. Soc. Chem.* **2005**, *127*, 7686–7687; g) Z. Lu, M. Yuan, F. Pan, S. Gao, D. Zhang, D. Zhu, *Inorg. Chem.* **2006**, *45*, 3538–3548.

[7] a) N. Weibel, L. J. Charbonnière, M. Guardigli, A. Roda, R. Ziessel, *J. Am. Chem. Soc.* **2004**, *126*, 4888–4896; b) J.-C. G. Bünzli, C. Piguet, *Chem. Soc. Rev.* **2005**, *34*, 1048–1077; c) J.-C. G. Bünzli, *Acc. Chem. Res.* **2006**, *39*, 53–61; d) P. Caravan, *Chem. Soc. Rev.* **2006**, *35*, 512–523; e) W. Radecka-Paryzek, V. Patroniak, J. Lisowski, *Coord. Chem. Rev.* **2005**, *249*, 2156–2175.

[8] W. Radecka-Paryzek, I. Pospieszna-Markiewicz, M. Kubicki, *Inorg. Chim. Acta* **2007**, *360*, 488–496.

[9] a) A. B. P. Lever, E. Mantovani, B. S. Ramaswamy, *Can. J. Chem.* **1971**, *49*, 1957–1964; b) L. Jin, D. Plancherel, J.-C. G. Bünzli, *Inorg. Chim. Acta* **1988**, *144*, 269–273; c) Y. Fukuda, A. Nakao, K. Hayashi, *J. Chem. Soc., Dalton Trans.* **2002**, 527–533.

[10] M. T. Kaczmarek, R. Jastrząb, E. Hołderna-Kędzia, W. Radecka-Paryzek, *Inorg. Chim. Acta* **2009**, *362*, 3127–3133.

[11] A. Mondry, K. Bukietyńska, *J. Alloys Compd.* **2004**, *374*, 27–31.

[12] V. Patroniak, M. Kubicki, A. Mondry, J. Lisowski, W. Radecka-Paryzek, *Dalton Trans.* **2004**, 3295–3304.

[13] R. Janicki, P. Starynowicz, A. Mondry, *Eur. J. Inorg. Chem.* **2008**, 3075–3082.

[14] Oxford Diffraction. *CrysAlis PRO* (Version 1.171.33.36d), Oxford Diffraction Ltd., **2009**.

[15] A. Altomare, G. Cascarano, C. Giacovazzo, A. Gualardi, *J. Appl. Crystallogr.* **1993**, *26*, 343–350.

[16] G. M. Sheldrick, *Acta Crystallogr., Sect. A* **2008**, *64*, 112–122.

Received: November 6, 2009
Published Online: March 31, 2010

 © 2010 Wiley-VCH Verlag GmbH & Co. KGaA, Weinheim